Research Article | Vol. 28, No. 11 / 25 May 2020 / Optics Express 16280
Optics EXPRESS

Opal-templated films for optical strain sensing

NONTHANAN SITPATHOM,[1,2] TANYAKORN MUANGNAPOH,[3] AND JUDITH M. DAWES[1,*]

[1]MQ Photonics, Department of Physics and Astronomy, Macquarie University, Sydney 2109, Australia
[2]Department of Physics, Faculty of Science, Mahidol University, Bangkok 10400, Thailand
[3]National Nanotechnology Center, Klong Luang, Pathumthani 12120, Thailand
[*]judith.dawes@mq.edu.au

Abstract: A polydimethylsiloxane film patterned by a self-assembled array has been demonstrated as a strain sensor. A monolayer of 580 nm polystyrene spheres prepared by convective deposition was the template to transfer a periodic pattern to a polydimethylsiloxane (PDMS) film. Optical diffraction through the stretched PDMS film, enabled strain sensing perpendicular and parallel to the stretching direction, with sensitivities of 1.7 nm/% strain and 4.0 nm/% strain, respectively. The PDMS film was used as a vibration sensor at 50 Hz.

1. Introduction

The optical reflection or transmission of photonic crystals is tunable by changing the period of the photonic crystal, leading to applications for wearable medical devices [1,2] mechanical sensing [3,4], pressure sensing [1,5], color filters [6], biomimetic tunable structural color [7], photoluminescence control [3], deformable contact lenses [8], optical diffusers [9], and anti-reflection coatings [10]. The period of the photonic crystal can be changed by mechanical stress [11] or electrical voltage [12] or heating [13]. The physical change can be sensed by measuring electrical properties [2,14], absorbed or reflected light [14,15] or both optical and electrical responses [4]. With no electrical contacts, optical strain sensors have potential for monitoring stress on skin [2,16].

Strain sensors may be one, two, or three-dimensional photonic crystals [17], fabricated by electron beam etching [18], photolithography [19], micro-printing [20] or self-assembly [21,22]. Photolithography and electron beam etching provide precise patterning, but low-cost fabrication of large area sensors is more readily achieved with colloidal self-assembly by spin coating [23], dip coating [24] or vertical deposition [25]. Convective deposition [26,27] with substrate vibration [28] is economical, requiring less colloidal solution, and creates highly ordered structures.

The performance of flexible photonic crystal sensors depends on their geometry and composition. For example, gold nanoparticles aligned in a one-dimensional metamaterial array provided an almost linear sensing response [29]. However, a one-dimensional grating produces a broadband zero diffraction order beam (increasing the background) and senses in a single strain direction. Structures with crossed gratings on both sides of an elastomeric sheet [30], or 2D gratings using photonic crystals, [15] can sense in multiple directions.

Strain sensors fabricated from colloidal self-assembly processes can be two- or three-dimensional structures, such as a face-centred cubic arrangement of microspheres, filled by polydimethylsiloxane (PDMS) [22] or polymer gel [31]. PDMS infiltration into opal can disrupt the array due to the viscosity of the precursor. Irregular cracking of the spheres and matrix may also arise under strain. Patterning using a monolayer is a practical solution to these problems. To investigate mechanical strain, changes in Bragg diffraction measure compression thickness [31] or stretched length [22]. In order for optical strain sensors to be useful, the period of the relevant grating must diffract visible light efficiently, according to the Bragg diffraction equation,

#390095 https://doi.org/10.1364/OE.390095
Journal © 2020 Received 11 Feb 2020; revised 5 Apr 2020; accepted 5 May 2020; published 14 May 2020

Optics EXPRESS

$d(\sin\theta_m - \sin\theta_i) = m\lambda$ where d is the grating period, and θ_m, θ_i, m and λ represent the diffracted and incident angles, the diffraction order and wavelength of the light, respectively.

When simultaneously sensing mechanical strain in two orthogonal directions, the Poisson effect, in which stress and strain in one direction are coupled to those in orthogonal directions, must be considered. The Poisson ratio is the ratio of the longitudinal and transverse strains under an applied force. The mechanical properties of PDMS depend on factors such curing temperature [32] and the mixing ratio of polydimethylsiloxane base and curing agent [33–37]. The Poisson ratio for PDMS varies from 0.4 to 0.58, depending on preparation methods, the chosen definition [35] and film thickness [36]. The Poisson ratio depends on the measurement time (due to molecular relaxation [35]) and may vary with inhomogeneous mixing [35]. After repeated stresses, the polymer chains can relax to different zero-strain states [36]. The approach taken by Kim *et al.*, [38] removes the complication of the Poisson effect by transversely pre-stressing the sensor to ensure a reliable measurement in the stretching direction.

Here we report an omnidirectional strain sensor, which uses optical measurement of the strain in two directions. Using a polystyrene microsphere monolayer as our template, we fabricated strain sensors in polydimethylsiloxane, (PDMS), which is nontoxic, optically transparent, and tolerant to repeated stress, up to 213% strain [39]. Fabrication is efficient, with only a few steps. The strain response and sensitivity of the sensors were optically characterized by diffraction for the different crystal axes vs stretch direction. Using the calibrated sensor response in two orthogonal directions, we can analyze the diffracted light to measure the parallel and perpendicular strain resulting from an applied stress. We measured the device's reproducibility and its response to vibrations.

2. Fabrication and measurement

2.1. Patterned polydimethylsiloxane film preparation

Two-dimensional close-packed hexagonal arrays of polystyrene spheres were prepared by convective deposition, a self-assembly process, on horizontal glass substrates. The substrates, microscope slides, were first cleaned ultrasonically in isopropanol. The monolayer of polystyrene spheres (Bang Laboratories, diameter 580 nm, <3% CV) was prepared at room temperature, relative humidity of 65%. The suspension (10 µL) was dropped into a gap between a glass slide fixed at 45° and the glass substrate, and the substrate was slowly moved away from the glass blade to facilitate the monolayer formation with speed of 28 µm/s. During the coating process, a mechanical wave driver [28] vibrated the substrate with a sinusoidal oscillation of 40 Hz to reduce the particle aggregation and facilitate the formation of an ordered monolayer. Typically, the coating direction controls the orientation of the photonic crystal, and the resulting domains are well-aligned as shown in Fig. 2. The PDMS matrix was prepared from a two-part mix of curing agent and base (Sylgard 184 Silicon Elastomer kit). The mixture (1:10 ratio of curing agent: base) was dropped on the polystyrene array and left to stand until it cured. The patterned PDMS films had an area of 2.5 cm x 2.5 cm with thickness of 0.76 ± 0.05 mm. Finally, after polymerization was complete, the PDMS film was peeled carefully away from the polystyrene monolayer. The surface of the patterned PDMS film has vacancies from the polystyrene spheres, and the lower surface is flat. The fabrication of the polystyrene monolayer and the patterned PDMS film are shown schematically in Figs. 1(a)–1(c) and the optical diffraction measurement is shown schematically in Fig. 1(d). Figures 2(a)–2(b) show scanning electron micrographs of the microsphere array and the PDMS imprinted with an array of voids.

2.2. Characterization

Mechanical strain sensing of the patterned PDMS films was measured and analyzed with respect to two orientations of the films. The two sides of the film were glued to microscope slides

Optics EXPRESS

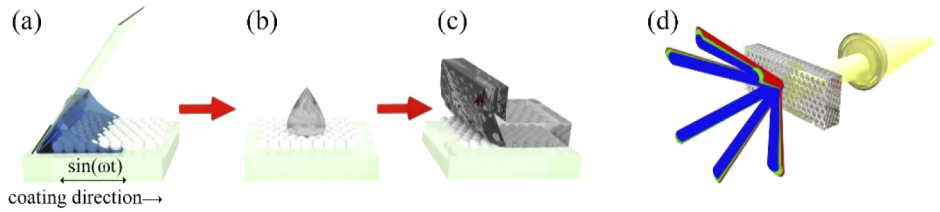

Fig. 1. Fabrication: (a) convective deposition on a glass substrate (b) dropping PDMS mixture on the polystyrene sphere monolayer (c) removing the patterned PDMS film and (d) transmitted diffracted light.

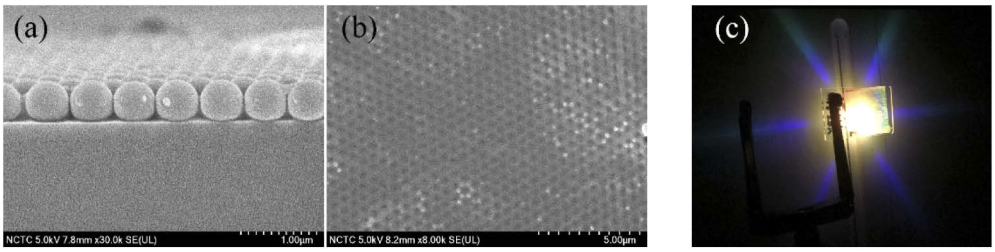

Fig. 2. Scanning electron micrographs of (a) monolayer of 580 nm polystyrene spheres in cross-section and (b) top view of the patterned PDMS film, and (c) optical diffraction from the PDMS film.

which were held using clamps, and the film was stretched by pulling one side with a micrometer. The film was illuminated by a white light source based on a fiber-coupled halogen lamp, and the diffracted light was measured in transmission using a fiber-coupled spectrometer. First, the coating direction of the PDMS film was orthogonal to the stretched direction. Second, the PDMS film was rotated by 90° to align the coating direction along the stretching direction. In addition, the PDMS film was employed as a vibration sensor. The frequency measurement was designed by attaching the film at one end to a balsa wood holder attached to an audio loudspeaker while the opposite end of the film was fixed. The film was illuminated by a diode laser with wavelength of 405 ± 10 nm. The diffracted light from the vibrating PDMS film was detected by a fixed photodiode connected to an oscilloscope, to determine the vibration frequency of the sensor. The electrical drive signal was monitored as a reference.

3. Results and discussion

The PDMS strain sensor was modeled using the grating equation in Section 1, where the diffracted wavelength depends on the grating period, d, for fixed angles of incidence and diffraction. When the film is stretched by mechanical stress, the diffracted wavelength changes as a function of angle. Thus, different diffracted colors are seen under applied stress. Figure 2(c) shows light (410 to 580 nm) diffracted from the PDMS film at angles of 45° to 90°, showing its hexagonal symmetry. The characteristic axes for a close-packed-hexagonal array of spheres are oriented at 60° to each other. Considering the lattice period of the array perpendicular to the coating direction, the distance between the center of a particle and that of its second nearest neighbor, ax_1 is $\sqrt{3}d$ where d is the sphere diameter. The other lattice constant is d, the spacing between nearest neighbors, along the coating direction, ax_2. Hence ideal hexagonal arrays of 580 nm spheres should display characteristic periods of 1004 nm and 580 nm, in orthogonal directions. The period of the polystyrene monolayer was fitted to the measured optical diffraction spectra for angles from 60° to 80° in the two orthogonal axes, and along the direction parallel to the

Optics EXPRESS

coating axis, the observed period was 582 ± 29 nm. Perpendicular to the coating direction, the monolayer lattice period was 599 ± 14 nm, (the expected period is 580 nm). The patterned PDMS film had an effective lattice period of 400 ± 76 nm in the coating direction (measured in third order diffraction) and 576 ± 48 nm perpendicular to the coating direction, with differences from ideal packing of 20% and 0.7% parallel and perpendicular to the coating direction, respectively. Discrepancies in the lattice period of the PDMS films were greater than for the polystyrene sphere arrays, due to distortions of the shape and surface of the polymer film. In contrast, the polystyrene sphere monolayer on the glass substrate is highly ordered, with a flat surface, because the highly monodisperse microspheres were deposited on a flat substrate. Multiple sensors were fabricated with similar properties, and the optical response was consistent across the area of the films.

To analyze sensing ability, diffraction under increasing mechanical stress from 0 to 10% in a direction perpendicular to the stretched direction, was measured at a fixed photo-detector position (see Fig. 3(a)). The transmitted diffraction spectra from the PDMS sensor are shown in Figs. 3(a) and 3(b). The diffracted wavelength of the PDMS sensor without stretch was

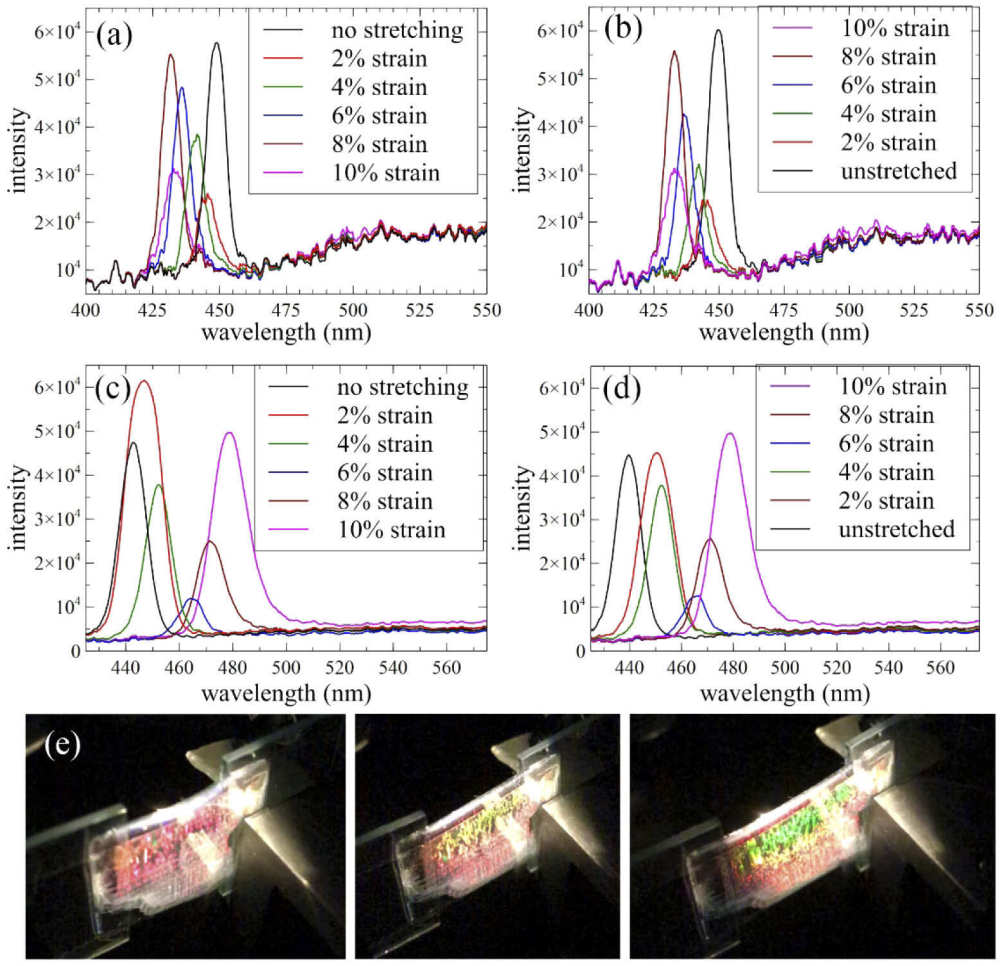

Fig. 3. Optical diffraction spectra from the stretched PDMS sensor, measured (a, b) perpendicular to the stretching direction (c, d) parallel to the stretching direction, for (a, c) increasing strain, and (b, d) decreasing strain, (e) photos of the PDMS sensor observed under increasing mechanical strain.

Optics EXPRESS

448 ± 3 nm, and at 10% strain, the intensity peak (434 ± 5 nm) shifted 3% from the original. Figure 3(b) shows the spectra recorded for decreasing stretching, relaxing from 10% applied strain to zero strain, with the final peak at 450 ± 4 nm. The peaks shift to shorter wavelength under perpendicular mechanical stress due to the Poisson effect. The optical diffraction spectra parallel to the stretching direction vs applied strain for increasing stretching and then decreasing stretching, are shown in Figs. 3(c) and 3(d), respectively. As expected, the peak moved to longer wavelength for increased stress. The peak diffracted wavelength was 441 ± 4 nm for zero strain and 478 ± 5 nm for 10% strain. For this axis, the diffracted wavelength at 10% strain increased by 8% from the wavelength with zero strain. After returning to zero strain, the final peak was 439 ± 4 nm.

The PDMS sensor was rotated by 90° so that it was stretched along the coating direction. We again measured the strain sensing performance both perpendicular and parallel to the stretching direction. The optical response of the film observed perpendicular to the stretched axis changed negligibly, implying that this was aligned with ax_2, the particle-particle distance. Thus, it would not change as the air holes came together, due to the Poisson effect. The optical spectra along the stretched direction show greater changes with mechanical strain. Under an applied strain of 0 to 10%, the diffracted wavelength varied from 430 ± 3 nm to 468 ± 5 nm, and relaxed back to 428 ± 4 nm at zero strain.

The sensitivity of the strain sensor, the change of wavelength per percent strain, was fitted from the spectra: in the perpendicular direction, the increased stretching sensitivity was 1.7 ± 0.5 nm/% strain, (black line in Fig. 4(a)) while the sensitivity of decreased stretching was 1.8 ± 0.5 nm/% strain (red line in Fig. 4(a)). The sensitivity of strain sensing in the parallel direction, shown in Fig. 4(b), was found to be 3.9 ± 0.5 nm/% strain and 4.0 ± 0.6 nm/% strain for the increasing and decreasing directions, respectively. A slight hysteresis was observed with decreasing stretching, possibly due to polymer relaxation [35]. The PDMS sensor's sensitivity in the stretching direction parallel to the coating direction was 4.0 ± 0.5 nm/% strain and 4.0 ± 0.6 nm/% strain, for increased and decreased stretching, respectively. No sensitivity for the perpendicular axis was determined. By combining information on the two directions of strain for a given stress, we are able to determine the direction of the applied stress. The calibrated response of the sensor in the parallel and perpendicular directions can be compared to determine the components of the stress and strain in each direction.

Using similar flexible strain sensors, under compression, Iwayama *et al.*, [31] detected a sensitivity of 6.0 nm/% strain and Ito *et al.*, [40] detected a sensitivity of 5.5 nm/% strain, whereas Piccolo *et al.*, [15] found sensitivities of 4.5 ± 0.1 nm/% strain and 2.5 ± 0.1 nm/% strain for sensing tensile strain parallel and at 60° to the stretch direction. Differences in sensitivity for these sensors may be explained because the period of the opal template and the wavelength range of operation influence detection of diffraction at first or higher orders, which affects the sensitivity. While we used 580 nm spheres, with visible light to observe third order diffraction, larger periods (such as the 1.6 µm polystyrene sphere array used by Piccolo *et al.*, [15]) would allow improved sensitivity at first order diffraction. The sensitivity of the strain sensor is greater in the direction parallel to the stretch than that perpendicular, because the imposed strain governs the sensor response in the direction parallel to the stretch, but in the perpendicular direction, the detected change is due to the Poisson effect [15]. The thickness and width of the film under stretching are both changed due to the Poisson effect, but the thickness is not likely to affect the optical diffraction pattern as it is expected to be a uniform thickness change throughout the PDMS film. The Poisson ratio for our PDMS films was calculated as the ratio of tensile strain to transverse strain and found to be 0.59 ± 0.2, compared with reported values of 0.42 to 0.58 [32,33]. The experimental Poisson ratio depends on the mixing ratio of base and curing agent, curing conditions, and the surface profile of the film. The capacity of the patterned PDMS film

Optics EXPRESS

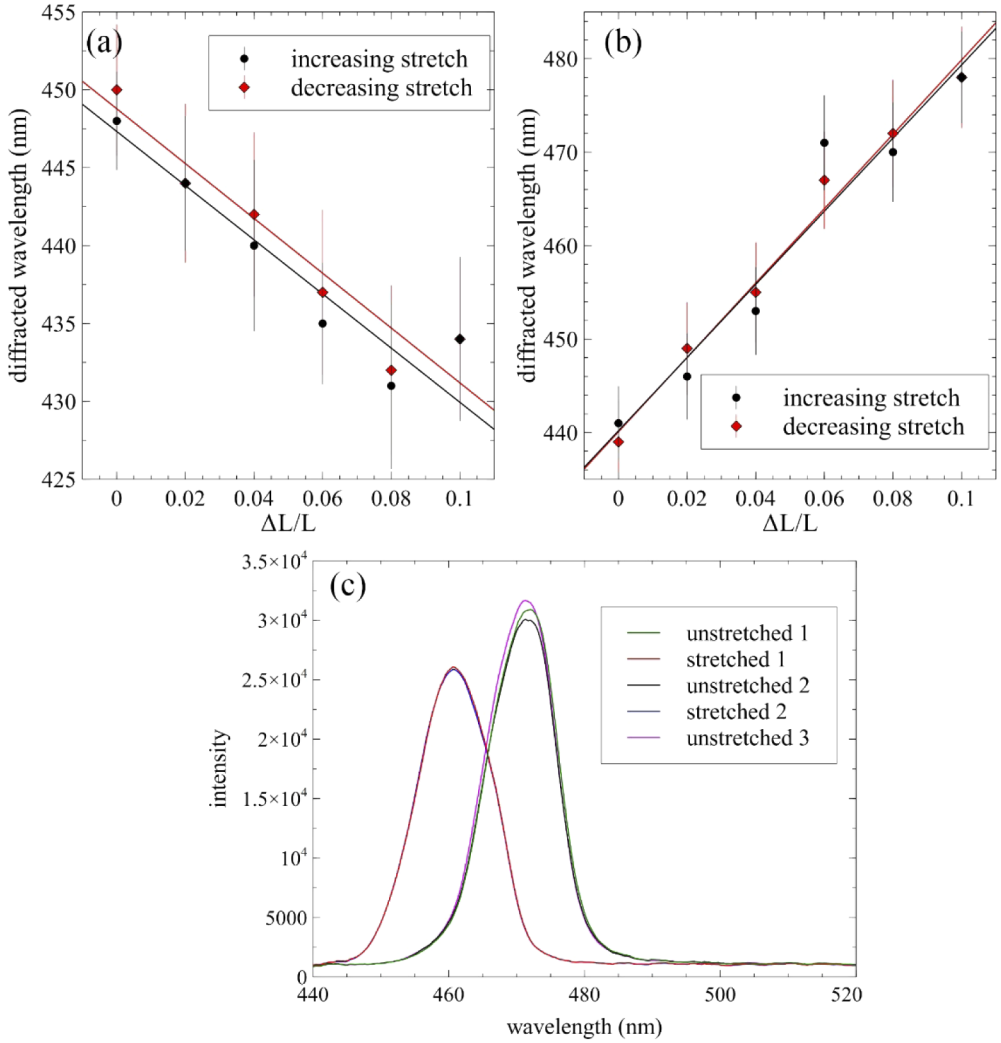

Fig. 4. Graph of mechanical strain vs diffracted wavelength for measurement (a) perpendicular and (b) parallel to the stretching direction, which was perpendicular to the original coating direction, and (c) cyclic measurement of transmitted wavelength.

as a force sensor was determined to be in the range of 3 N, estimated using Young's modulus of 2.61 [36] and the measured film thickness of 0.76 ± 0.05 mm.

The opal films that are produced by convective deposition have a preferred direction for their domains [25–27], but the drying process tends to introduce defects such as cracks in the monolayers. By analyzing scanning electron micrographs of some of the opal templated films, we observed that typically the defects arise as gaps of about 10-30 nm between regularly aligned domains of 5-10 periods. On conducting simulations of the diffracted spectra from domains incorporating these small defects, we see shifts of the diffracted peak by 0.7 to 1.3% from that for the regular grating period of 580 nm. Thus, we anticipate that such defects would lead to around 1% error in the detected shifts.

Repeated cycles of stretching and relaxing are shown in Fig. 4(c). The peak diffracted wavelengths were highly reproducible: 473 nm, 472 nm and 472 nm for 0% stress, and 461 nm

Optics EXPRESS

and 461 nm for 10% stress, and the spectral profile was preserved. This is in contrast to the hysteresis observed in some strain sensors [14,41]. When the PDMS sensor was attached to a loudspeaker, the vibration frequency of the speaker was recovered in the photo-detector signal. The period detected using the PDMS sensor was 20.0 ms, corresponding to a frequency of 50.0 Hz, which was well-correlated with the drive signal at 49.5 Hz.

4. Conclusions

Mechanical strain sensors were fabricated with a low-cost, robust technique, imprinting a polydimethylsiloxane (PDMS) film by a hexagonal array of polystyrene spheres. The patterned PDMS film responded to applied mechanical stress in two orthogonal axes consistent with Poisson's ratio. The sensitive and reproducible detection of strain in orthogonal directions simultaneously to allow characterization of stress in 2D, is a key advantage of this two-dimensional grating structure.

Funding

Australian Research Council (DP160103332); Thailand Development and Promotion of Science and Technology Talent Program.

Acknowledgments

David Inglis and Danny Cochran are thanked for lending equipment. Part of this work was presented at the Asia Pacific Optical Sensing Conference in 2019.

Disclosures

The authors declare no conflicts of interest.

References

1. Y. Zhang, Y. Hu, P. Zhu, F. Han, Y. Zhu, R. Sun, and C.-P. Wong, "Flexible and Highly Sensitive Pressure Sensor Based on Microdome-Patterned PDMS Forming with Assistance of Colloid Self-Assembly and Replica Technique for Wearable Electronics," ACS Appl. Mater. Interfaces **9**(41), 35968–35976 (2017).
2. M. Amjadi, K. Kyung, I. Park, and M. Sitti, "Stretchable skin-mountable and wearable strain sensors and their potential applications: a review," Adv. Funct. Mater. **26**(11), 1678–1698 (2016).
3. A. Arsenault, T. J. Clark, G. V. Freymann, L. Cademartiri, R. Sapienza, J. Bertolotti, E. Vekris, S. Wong, V. Kitaev, I. Manners, R. Z. Wang, S. John, D. Wiersma, and G. A. Ozin, "From colour fingerprinting to the control of photoluminescence in elastic photonic crystals," Nat. Mater. **5**(3), 179–184 (2006).
4. P. Snapp, P. Kang, J. Leem, and S. Nam, "Colloidal photonic crystal strain sensor integrated with deformable graphene phototransducer," Adv. Funct. Mater. **29**(33), 1902216 (2019).
5. P. Escudero, J. Yeste, C. Pascual Izarra, R. Villa, and M. Alvarez, "Color tunable pressure sensors based on polymer nanostructured membranes for optofluidic applications," Sci. Rep. **9**(1), 3259 (2019).
6. H. Cho, S. Han, J. Kwon, J. Jung, H.-J. Kim, H. Kim, H. Eom, S. Hong, and S. H. Ko, "Self-assembled stretchable photonic crystal for a tunable color filter," Opt. Lett. **43**(15), 3501–3504 (2018).
7. H. Fudouzi, "Tunable structural color in organisms and photonic materials for design of bioinspired materials," Sci. Technol. Adv. Mater. **12**(6), 064704 (2011).
8. K. Min, S. Kim, and S. Kim, "Deformable, conformal silk hydrogel inverse opal," Proc. Natl. Acad. Sci. U. S. A. **114**(24), 6185–6190 (2017).
9. S. Mahpeykar, Q. Xiong, J. Wei, L. Meng, B. K. Russell, P. Hermansen, A. Singhal, and X. Wang, "Stretchable Hexagonal Diffraction Gratings as Optical Diffusers for In Situ Tunable Broadband Photon Management," Adv. Opt. Mater. **4**(7), 1106–1114 (2016).
10. A. Halder, M. S. Reddy, and R. Vijaya, "Enhancement of light collection through flexible polymeric films patterned using self-assembled photonic crystals," J. Phys. D: Appl. Phys. **48**(26), 265103 (2015).
11. H. Fudouzi and Y. Xia, "Colloidal crystals with tunable colors and their use as photonic papers," Langmuir **19**(23), 9653–9660 (2003).
12. T. Yin, D. Zhong, J. Lie, X. Liu, H. Yu, and S. Qu, "Stretch tuning of the Debye ring for 2D photonic crystals on a dielectric elastomer membrane," Soft Matter **14**(7), 1120–1129 (2018).
13. N. Sharac, H. Sharma, M. Veysi, R. N. Sanderson, M. Khine, F. Capolino, and R. Ragan, "Tunable optical response of bowtie nanoantenna arrays on thermoplastic substrates," Nanotechnology **27**(10), 105302 (2016).

Optics EXPRESS

14. C. Minnai, M. D. Vece, and P. Milani, "Mechanical-optical-electro modulation by stretching a polymer-metal nanocomposite," Nanotechnology **28**(35), 355702 (2017).
15. V. Piccolo, A. Chiappini, C. Armellini, M. Barozzi, A. Lukowiak, P. A. Sazio, A. Vaccari, M. Ferrari, and D. Zonta, "2D optical gratings based on hexagonal voids on transparent elastomeric substrate," Micromachines **9**(7), 345 (2018).
16. H. Park, D. S. Kim, S. Y. Hong, C. Kim, J. Y. Yun, S. Y. Oh, S. W. Jin, Y. R. Jeong, G. T. Kim, and J. S. Ha, "A skin integrated transparent and stretchable strain sensor with interactive color changing electrochromic displays," Nanoscale **9**(22), 7631–7640 (2017).
17. K. Yoshino, Y. Kawagishi, M. Ozaki, and A. Kose, "Mechanical tuning of the optical properties of plastic opal as a photonic crystal," Jpn. J. Appl. Phys. **38**(Part 2, No. 7A), L786–L788 (1999).
18. H. Kumagai, H. Honma, M. Ishida, K. Sawada, and K. Takahashi, "Fabrication of a thin plasmonic color sheet embedded with Al subwavelength gratings in parylene," Displays **45**, 63–69 (2016).
19. X. Zhang, J. Zhang, H. Liu, X. Su, and L. Wang, "Soft plasmons with stretchable spectroscopic response based on thermally patterned gold nanoparticles," Sci. Rep. **4**(1), 4182 (2015).
20. L. Minati, A. Chiappini, C. Armellini, A. Carpentiero, D. Maniglio, A. Vaccari, L. Zur, A. Lukowiak, M. Ferrari, and G. Speranza, "Gold nanoparticles 1D array as mechanochromic strain sensor," Mater. Chem. Phys. **192**, 94–99 (2017).
21. O. Purslainen, J. J. Baumberg, K. Ryan, J. Bauer, H. Winkler, B. Viel, and T. Ruhl, "Compact strain sensitive flexible photonic crystals for sensors," Appl. Phys. Lett. **87**(10), 101902 (2005).
22. H. Fudouzi and T. Sawada, "Photonic rubber sheets with tunable color by elastic deformation," Langmuir **22**(3), 1365–1368 (2006).
23. Z. Yi, G. Niu, J. Luo, X. Kang, W. Yao, W. Zhang, Y. Yi, Y. Yi, X. Ye, T. Duan, and Y. Tang, "Ordered array of Ag semishells on different diameter monolayer polystyrene colloidal crystals," Sci. Rep. **6**(1), 32314 (2016).
24. C. Garcia Nunez, W. Navaraj, F. Liu, D. Shakthivel, and R. Dahiya, "Large-Area Self-Assembly of Silica Microspheres by Temperature-Assisted Dip-Coating," ACS Appl. Mater. Interfaces **10**(3), 3058–3068 (2018).
25. J. Meijer, F. Hagemans, L. Rossi, D. V. Byelov, S. I. R. Castillo, A. Snigirev, I. Snigireva, A. P. Philipse, and A. V. Petukhov, "Self-Assembly of Colloidal Cubes via Vertical Deposition," Langmuir **28**(20), 7631–7638 (2012).
26. K. Joshi, T. Muangnapoh, M. D. Stever, and F. Gilchrist, "Effect of Ionic Strength and Surface Charge on Convective Deposition," Langmuir **31**(45), 12348–12353 (2015).
27. P. Kumnorkaew and J. F. Gilchrist, "Effect of Nanoparticle Concentration on the Convective Deposition of Binary Suspensions," Langmuir **25**(11), 6070–6075 (2009).
28. T. Muangnapoh, A. L. Weldon, and J. F. Gilchrist, "Enhanced colloidal monolayer assembly via vibration-assisted convective deposition," Appl. Phys. Lett. **103**(18), 181603 (2013).
29. W. Wu, M. Ren, B. Pi, Y. Wu, W. Cai, and J. Xu, "Scaffold metamaterial and its application as strain sensor," Appl. Phys. Lett. **107**(9), 091104 (2015).
30. H. Guo, J. Tang, K. Qian, D. Tsoukalas, M. Zhao, J. Yang, B. Zhang, X. Chou, J. Liu, C. Xue, and W. D. Zhang, "Vectorial strain gauge method using single flexible orthogonal PDMS gratings," Sci. Rep. **6**(1), 23606 (2016).
31. X. Huang, M. Bjork, D. C. Ratchford, and J. Yeom, "Pitch control of hexagonal non-close packed nanosphere arrays using isotropic deformation of an elastomer," Langmuir **33**(43), 12218–12226 (2017).
32. Y. Iwayama, J. Yamanaka, Y. Takiguchi, M. Takasaka, K. Ito, T. Shinohara, T. Sawada, and M. Yonese, "Optically tunable gelled photonic crystal covering almost the entire visible light wavelength region," Langmuir **19**(4), 977–980 (2003).
33. R. Seghir and S. Arscott, "Extended PDMS stiffness range for flexible systems," Sens. Actuators, A **230**, 33–39 (2015).
34. K. Khanafer, A. Duprey, M. Chlicht, and R. Berguer, "Effects of strain rate, mixing ratio, and stress-strain definition on the mechanical behavior of the polydimethylsiloxane (PDMS) material," Biomed. Microdevices **11**(2), 503–508 (2009).
35. T. K. Kim, J. K. Kim, and O. Jeong, "Measurement of nonlinear mechanical properties of PDMS elastomer," Microelectron. Eng. **88**(8), 1982–1985 (2011).
36. S. Dogru, B. Aksoy, H. Bayraktar, and B. Alaca, "Poisson's ratio of PDMS thin films," Polym. Test. **69**, 375–384 (2018).
37. M. Liu, J. Sun, Y. Sun, C. Bock, and Q. Chen, "Thickness-dependent mechanical properties of PDMS membranes," J. Micromech. Microeng. **19**(3), 035028 (2009).
38. K. K. Kim, S. Hong, H. M. Ho, J. Lee, Y. D. Suh, J. Ham, and S. H. Ko, "Highly sensitive and stretchable multidimensional strain sensor with prestrained anisotropic metal nanowire percolation networks," Nano Lett. **15**(8), 5240–5247 (2015).
39. W. Lee, K. Teo, A. Andriyana, Y. Shee, and F. Adikan, "Effect of cyclic compression and curing agent concentration on the stabilization of mechanical properties of PDMS elastomer," Mater. Des. **96**, 470–475 (2016).
40. T. Ito, C. Katsura, H. Sugimoto, E. Nakanishi, and K. Inomata, "Strain responsive structural colored elastomers by fixing colloidal crystal assembly," Langmuir **29**(45), 13951–13957 (2013).
41. B Viel, T. Ruhl, and G. P. Hellmann, "Reversible deformation of opal elastomers," Chem. Mater. **19**(23), 5673–5679 (2007).